



Simulation results for light propagation in the central detector: 2-dimensional case

A. F. Barbosa

Centro Brasileiro de Pesquisas Físicas - CBPF, e-mail: laudo@cbpf.br

Abstract

A simple simulation study of light propagation inside the central detector active volume has been done, aiming to evaluate the importance of reflecting inner surfaces. Photons are supposed to be point-like entities traveling in straight lines, and only a two dimensional section of the detection volume is taken into account. Half-circular and half-elliptic geometries for the photocathode in the photomultiplier tube (PMT) are considered, as well as different configurations of PMTs in the detector. The maximum number of photon reflections in the walls before collection in a PMT is varied, so that one may estimate the required attenuation length for a given efficiency of photon capturing. A light reflecting structure around the PMTs is also implemented in the simulation, in order to reduce the probability for a photon to be bounced back to the direction from which it was emitted.

1 Introduction

After safety considerations with the Angra II power plant administration, it has been decided that the anti-neutrino detector should be developed using water as the target material, instead of liquid scintillator. It has also been decided that the implementation should take place at the surface level, since a study of the risks brought by an underground installation would take long, and the probability for approval is low. On the other hand, the project has been granted the possibility to construct the detector very near the walls of the dome housing the reactor core. At this position, anti-neutrino flux per unit volume in the detector close to the highest possible.

This has led to a cubic design, to be fit into a container, instead of the previously planned cylindrical geometry. In Figure 1 a realistic view of the latest technical drawings for the central detector is shown. The one ton target volume is surrounded by 40 PMTs. Validation of this design requires some simulation work in order to verify, for example, whether it is mandatory or not to install PMTs in the vertical detector walls.

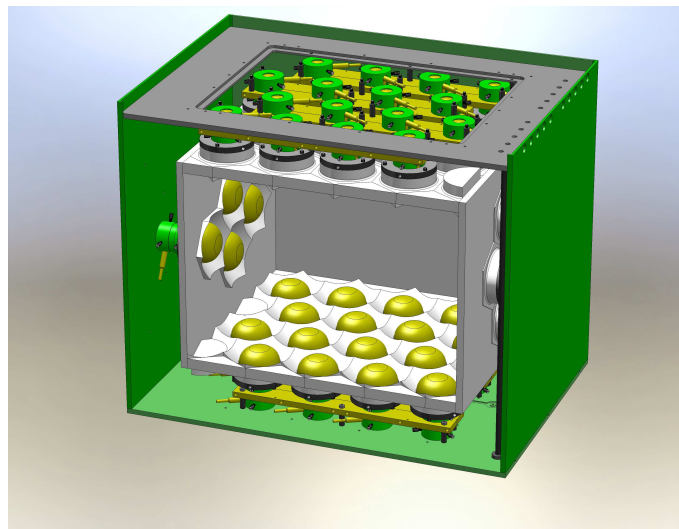


Figure 1: View of the latest technical drawing for the central detector.

In the present work we start to address the issue of photon collection efficiency. It seems clear that, for maximum signal amplitude after particle detection, one should implement a reflecting surface in the areas of the walls not occupied with PMTs. Moreover, the arrival direction of photoelectrons may be effectively used as a VETO technique, provided that the information on the emission direction is not lost. We aim at producing results that quantify these intuitive hints.

For this sake, we have written a very simple simulation code that represents photons as point-like entities traveling in straight lines inside the detector. Whenever a photon reaches a PMT surface it is considered detected. In case it reaches the walls, it may be either absorbed or reflected. The maximum number of reflections is programmable, and this allows one to estimate the required attenuation length for light propagation in water for optimal photon counting efficiency. The code is written in *C++* and compiled under *gcc/g++*. The visualization of photon trajectories is obtained with a *C++* script running under the *ROOT* (<http://root.cern.ch>) platform.

This work may represent a starting point for more detailed and realistic detector simulations, including the development of electric signals in the PMTs.

2 Trajectory parameters calculation

The photon trajectory is here described by the straight line equation:

$$y = Ax + B \quad (1)$$

The trajectory parameters are thus A and B . The cartesian coordinates y and x stand respectively for the position along the height and along the width of the two-dimensional box.

2.1 Photon capture in a PMT

The capture of a photon in a PMT is understood simply as the intersection of its trajectory, as defined above, and the function describing the PMT photocathode surface. In the general case, the latter is one of the halves of an ellipsis with radii a and b , centered at the position (x_o, y_o) , such that:

$$y = \frac{(x - x_o)^2}{a^2} + \frac{(y - y_o)^2}{b^2} \quad (2)$$

The particular case of a circular PMT is that with $a=b$. The intersection occurs at the positions $x_{1,2}$ along the x direction, as given by:

$$\left\{ \begin{array}{l} x_{1,2} = \frac{-\beta \pm \sqrt{\Delta}}{2\alpha} \\ \text{with:} \\ \Delta = \beta^2 - 4\alpha\gamma; \\ \alpha = A^2 + \frac{b^2}{a^2}; \\ \beta = 2A(B - y_o) - 2x_o \frac{b^2}{a^2}; \\ \gamma = (B - y_o)^2 + \frac{(bx_o)^2}{a^2} - b^2. \end{array} \right. \quad (3)$$

The $y_{1,2}$ coordinates for the intersection point may be obtained from $y_{1,2} = Ax_{1,2} + B$. Trajectories for which we have $\Delta < 0$ do not intercept the photocathode surface.

2.2 Reflection in the walls

A reflection may be interpreted as an operation that changes one trajectory to another:

$$Ax + B \longrightarrow A_r x + B_r \quad (4)$$

It is easy to see that, when the reflecting surface is horizontal or vertical, the angular coefficient for the reflected trajectory is $A_r = -A$. This corresponds to reflections in the detector walls. For the B_r parameter we find:

$$B_r = 2Ax_o + B \quad (5)$$

The (x_o, y_o) coordinates for the reflection point are given by:

$$\begin{aligned}
& \left(-\frac{B}{A}, 0\right), & \text{[lower wall]} \\
& \left(\frac{H-B}{A}, H\right), & \text{[upper wall]} \\
& (0, B), & \text{[left wall]} \\
& (L, AL + B), & \text{[right wall]}
\end{aligned} \tag{6}$$

In the equation above, H and L stand respectively for the height and the width of the detector active area.

2.3 Reflection in a rotated surface

In order to get the trajectory parameters (A_r and B_r) for a photon which is reflected in a flat surface that is not horizontal, but makes angle ξ with respect to it, we may start by looking at the reflection in the non-rotated surface. Then we first rotate the coordinate system by angle $-\xi$. Under this transformation, the trajectory parameters A and B are led to A_g and B_g , given by:

$$\begin{aligned}
A_g &= \frac{A \cos(\xi) + \sin(\xi)}{\cos(\xi) - A \sin(\xi)} \\
B_g &= \frac{B}{\cos(\xi) - A \sin(\xi)}
\end{aligned} \tag{7}$$

In the rotated coordinate system, the reflected trajectory has angular coefficient $A_{rg} = -A_g$ (because the reflecting surface is horizontal in this system). The A_r parameter for the trajectory in the original (non-rotated) system is obtained by rotating A_{rg} back by angle ξ :

$$\begin{aligned}
A_r &= \frac{A_{rg} \cos(\xi) - \sin(\xi)}{A \sin(\xi) + \cos(\xi)} \\
\therefore A_r &= \frac{A \cos(2\xi) + \sin(2\xi)}{A \sin(2\xi) - \cos(2\xi)}
\end{aligned} \tag{8}$$

In the last equation we have the A_r parameter, of the reflected trajectory in a rotated surface, as a function of the A parameter, of the incident trajectory. The B_r parameter may be obtained by requiring that the incident and reflected trajectories intercept at the reflection point, x_o , so that:

$$B_r = (A - A_r)x_o + B \tag{9}$$

3 Single PMT case

The simplest case treated here is that of a single PMT installed in a square box. The PMT is centered at the bottom of the box, which may feature 100% reflective or 100% absorbing inner walls. In Figure 2 are shown results of simulation for one thousand random events generated at the top surface of such a 2-dimensional box.

For the data shown in Figure 2, the photocathode is supposed to be half-circular, with radii 100mm or 200mm. The attenuation length for ultra pure water in the UV range is close to 100m. According to the results shown in Figure 2, nearly 90% of the photons would be detected by only one PMT in the box, provided that the walls are perfectly reflective and the water is transparent enough for the photons to undergo at least 10 (radius 200mm) or 20 (radius 100mm) reflections before reaching the photocathode. Adding more PMTs would clearly increase the detection efficiency.

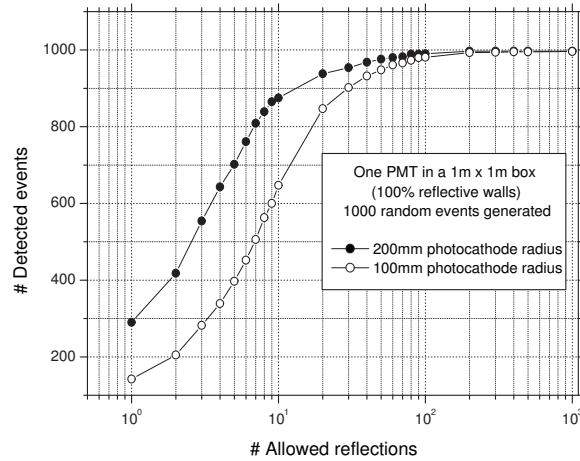


Figure 2: Number of detected events as a function of the number of allowed reflections.

The importance of having reflective walls is yet more evident when we consider completely absorbing walls, as illustrated in Figure 3. In this case, the fraction of detected photons for randomly generated photons at the detector top surface is only $\approx 10\%$ for the case of 200mm radius photocathode, and $\approx 6\%$ if this radius is 100mm.

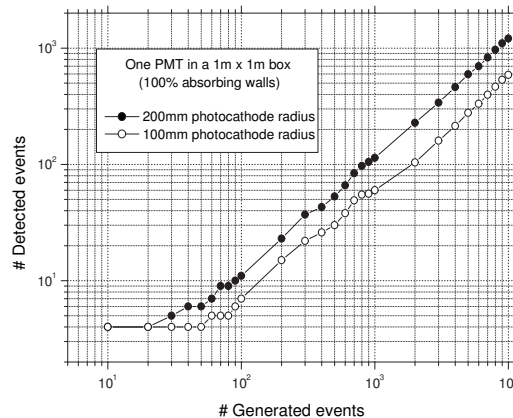


Figure 3: Detection efficiency for the case of absorbing detector walls.

The shape of the photocathode in the PMTs that will be used in the detector is not half-circular. It is better represented by a half-elliptic section, with radii 100mm (width) and 75mm (height). In Figure 4 are shown the data for perfectly reflective and perfectly absorbing walls for this particular case.

From Figure 4 we conclude that, for the PMTs actually used in the detector, over 30 reflections are required to insure 90% efficiency in photon capture. If the detector walls are perfectly absorbing this efficiency is $\approx 6\%$, as it was for the case of radius 100mm in Figure 3.

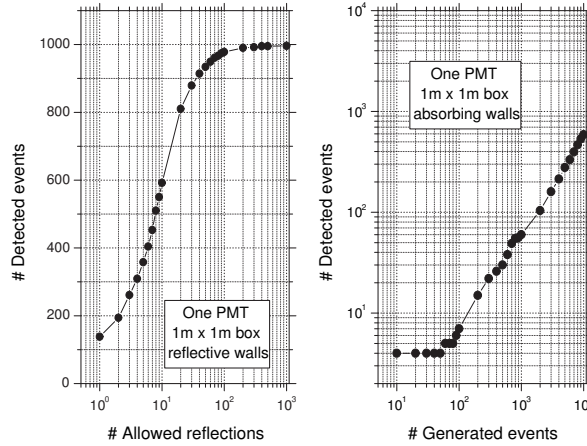


Figure 4: Results for a 200mm wide 75mm high photocathode.

4 Face-to-face and shifted PMTs

The results in the previous section suggest that, in order to efficiently capture the photons crossing the detector active volume, the inner walls should be reflective and covered with as many PMTs as possible. It is not feasible to cover the whole surface of the walls with PMTs, due to their round shape. The cost for an implementation with maximum coverage is also quite high. A compromise may be sought, balancing the number of PMTs and the reflective coating upon the walls, so that an acceptable efficiency is met.

In the Angra neutrino detector, one of the techniques to discriminate cosmic out of neutrino events relies on the fact that cosmic events mainly cross the detector from top to bottom. Since the photons are generated by the Cerenkov effect, the PMTs at the bottom are expected to see more photons per cosmic ray event than those at the top. The most basic configuration to take benefit on this feature is therefore the one with a set of PMTs at the top and another set at the bottom. It is true that cosmic events may be discriminated by other vetoing techniques. However, since the signal to background ratio is so low ($\approx 10^{-5}$), there is no harm in providing veto redundancy, and it may even be necessary for coping with neutrino events identification.

The configuration with 4 PMTs at the bottom directly facing 4 PMTs at the top is illustrated in Figure 5. The tracks of 100 random photons generated at the top surface are seen in the picture, with up to 10 reflections allowed before capture in a photocathode. The distance from one PMT to its nearest neighbor is 307mm, and the closest distance between photocathodes at the bottom and at the top is 0.9m, so that the area delimited by the PMTs is roughly 1m². Actually, this two-dimensional setup has PMTs delimiting an 1.28m × 0.9m area, which is a section of the planned detector target volume: 1.28m × 0.9m × 0.9m ($\approx 1m^3$).

In Figure 6 the main results for the 8 face-to-face PMTs configuration is shown. For reflective inner walls, more than 50% photon capture efficiency is obtained, even if only one reflection is allowed. With 5 reflections, the efficiency is above 90%. In case the inner walls absorb the photons instead of reflecting, the probability for photons to be captured in one of the PMTs is roughly 20%. Comparing Figures 4 and 6, we clearly see that the detector performance is improved by the reflective coating in the walls and by the addition of PMTs to cover more of the detecting surfaces.

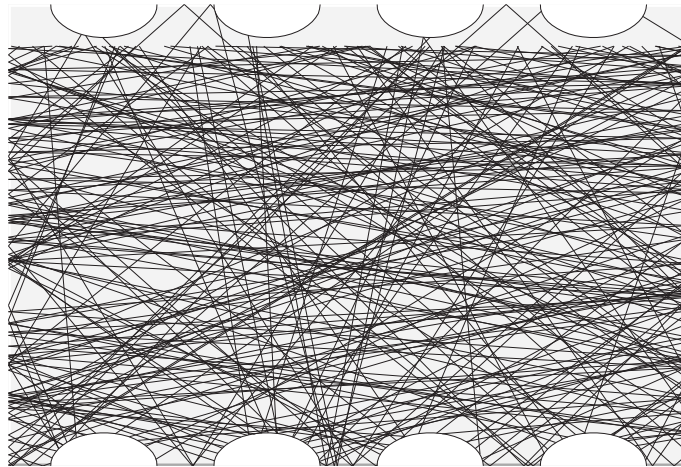


Figure 5: Illustration for the tracks of 100 random photons generated at the top of the detector (up to 10 reflections are allowed).

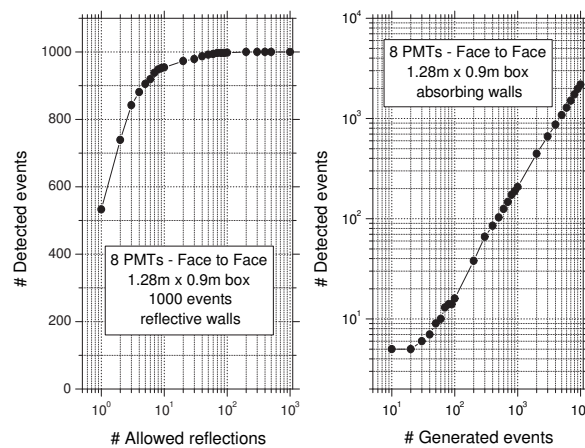


Figure 6: Photon capture efficiency for reflective (left) and absorbing (right) walls.

In order to estimate the sensitivity of the detector to identify the direction of the incoming photons, we may compute the fraction of photons detected at the bottom and at the top, for events generated at the top surface. From the data shown in Figure 7, on which this information is plotted, we find:

- If up to 5 reflections are allowed, the photon capture efficiency is $\approx 90\%$, and the fraction of top to bottom photons is $\approx 17\%$;
- If up to 10 reflections are allowed, the photon capture efficiency is $\approx 95\%$, and the fraction of top to bottom photons is still $\approx 17\%$;

We may as well look at a different configuration of PMTs and check whether the performance is changed. In Figure 8 is illustrated the case where the PMTs at the top and at the bottom are shifted, instead of being placed face to face.

The results for the case of the shifted PMTs configuration don't differ appreciably from what was found in the case of face-to-face PMTs, unless for the fact that the photon capture efficiency is slightly

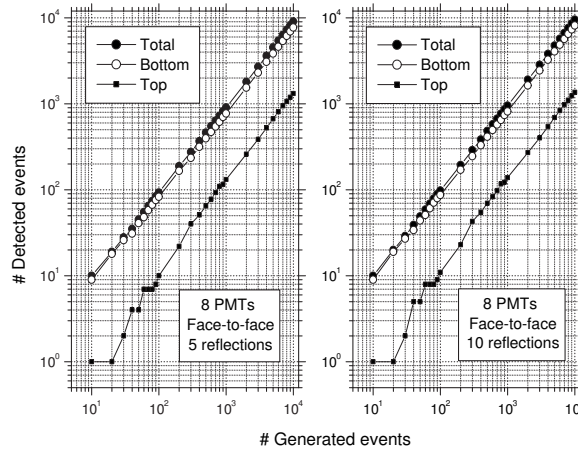


Figure 7: Photon capture efficiency at bottom and top surfaces for up to 5 (left) or 10 (right) allowed reflections.

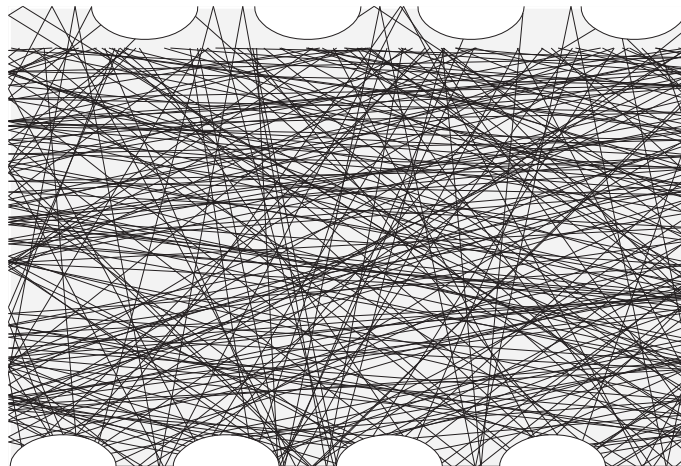


Figure 8: Illustration equivalent to Figure 5, with PMTs shifted.

better when more than 5 reflections are allowed. We find in the data that, in both configurations, $\approx 100\%$ of the photons are captured by the PMTs if 200 reflections are allowed.

Concerning the potentiality to identify the direction of the incoming photons, the analysis of the data in the cases of 5 and 10 allowed reflections for the configuration with shifted PMTs, shown in Figure 10, lead us to conclude:

- The photon capture efficiency is not appreciably changed, but the fraction of top to bottom photons is increased to $\approx 18\%$;

5 Reflecting structure around the PMTs

So far the presented results show that over 90% photon capture efficiency may be obtained with a relatively low PMT surface coverage combined with reflective coating of the inner walls. We would

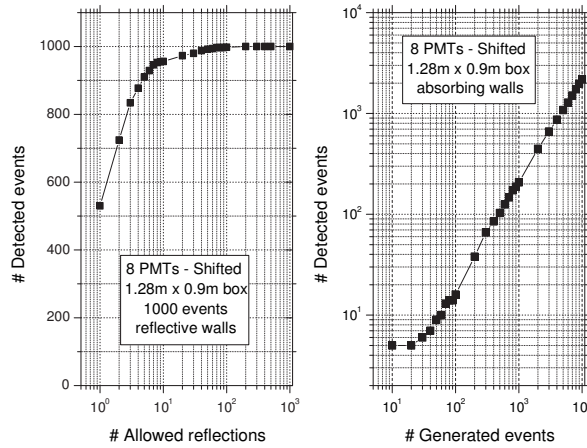


Figure 9: Graphs equivalent to Figure 6, with shifted PMTs.

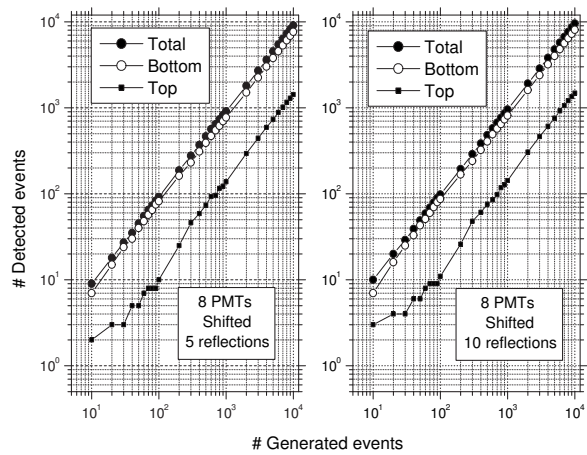


Figure 10: Graphs equivalent to Figure 7, with shifted PMTs.

also like to use the PMTs configuration to help identifying the direction of the incoming events, and we have found that, when the photons arrive from the top surface, the ratio of top to bottom detected photons is close to 20%. Supposing that photons from neutrino events are randomly distributed in the detector volume, there is a chance that we may exclude the events with unbalanced bottom to top ratio as non-related to neutrinos. However, since the total number of photoelectrons in neutrino events is low (well below 100 in average), statistical fluctuations may hinder this technique. It is therefore interesting to find a way to reduce the top to bottom photons ratio when the photons are known to arrive from the top. A possible solution is to provide a reflecting structure around the PMTs, so that photons hitting the surrounds of a PMT tend to be reflected into it. The simplest setup to implement for this purpose is perhaps the one illustrated in Figure 11.

The reflecting structures shown in Figure 11 are simply mirror planes placed side by side be-

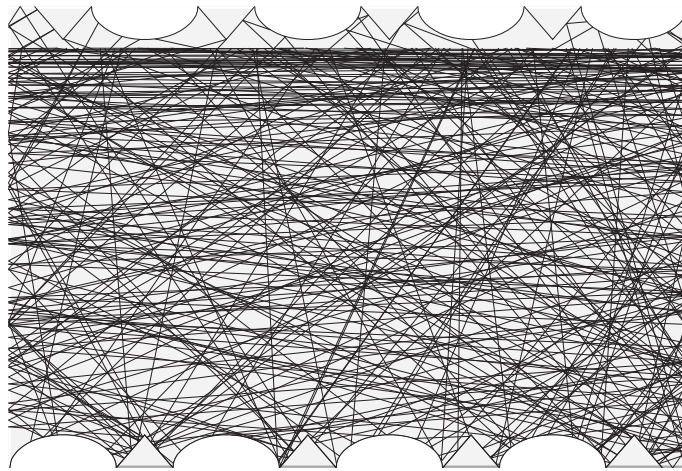


Figure 11: Illustration equivalent to Figures 5 and 8, with reflecting structures around the PMTs.

tween neighbor PMTs, at such an angle that they do not enter the active detecting area. In the three-dimensional case these would be similar to cones around the PMTs. The photon capture efficiency, for random photons generated at the top surface, is shown in Figure 12. We see that the efficiency is practically the same as that found for the other configurations (left side of Figures 6 and 9).

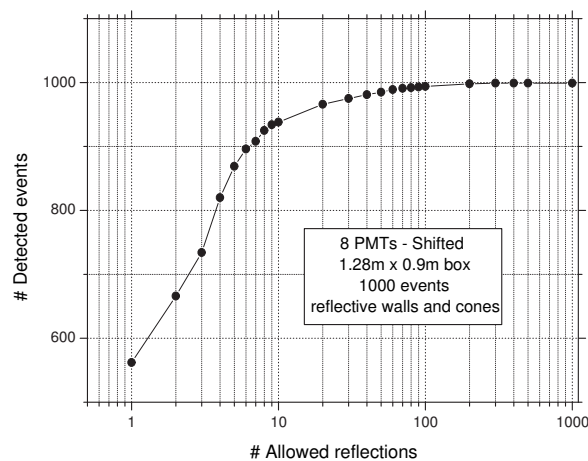


Figure 12: Photon capture efficiency, for PMTs surrounded by reflecting cones.

The ratio of top to bottom photons, for photons arriving from the top, is found NOT to be reduced by the introduction of the reflecting structures around the PTMs (at least not for the geometry shown in Figure 11). The results are presented in Figure 13, and may be summarized as follows:

- If up to 5 reflections are allowed, the photon capture efficiency is $\approx 85\%$, and the fraction of top to bottom photons is $\approx 22\%$;
- If up to 10 reflections are allowed, the photon capture efficiency is $\approx 94\%$, and the fraction of top to bottom photons is $\approx 26\%$;

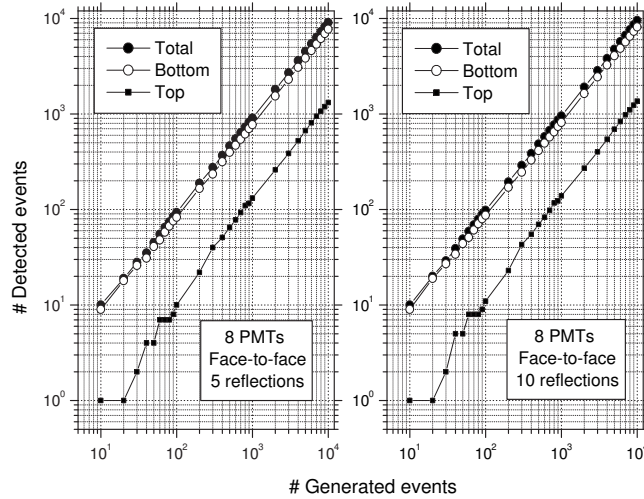


Figure 13: Equivalent to Figure 10, when the PMTs are surrounded by reflecting cones.

The introduction of the reflecting cones, therefore, does not necessarily improve the detector performance as expected. The reason for that, in the particular case of the simulated events, lies in the fact that the cones may as well act in the opposite sense: a photon arriving from the top can be reflected backwards due to the reflecting structures. In Figure 14 are shown the trajectories of a photon that happens to confirm this possibility after 10 reflections. We notice that such events are more likely when the angle determining the original photon direction (*i.e.*, the angular coefficient of the line related to the trajectory) is small.

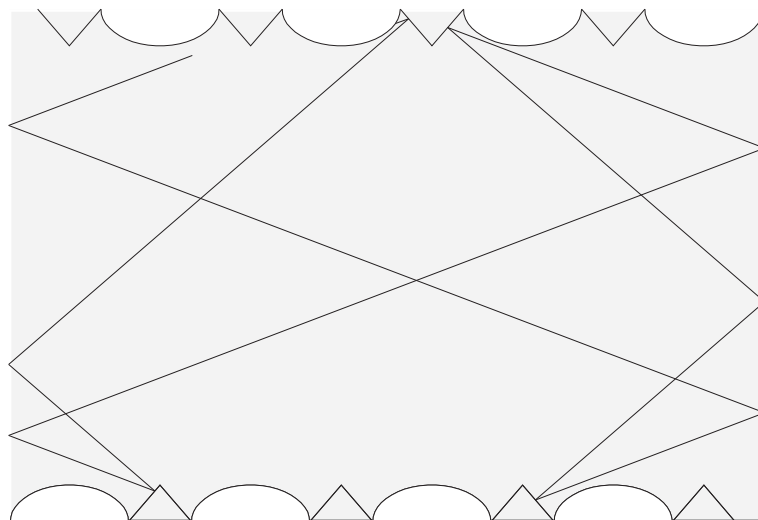


Figure 14: Illustration of a case where a photon arriving from the top is captured in one of the top PMTs.

5.1 Physical distribution for the direction of incident photons

For the above shown results, in order to generate the position of the events at the top surface of the detector, we have taken a random number from 0 to L ($L = 1280\text{mm}$ is the length of the two-dimensional box). The height was fixed to 20mm below the surface of the top PMT's photocathodes. For the direction, we took a random number from 0 to π , and associated it to the angular coefficient of the straight line defined by the photon trajectory, pointing downwards. The tracks so generated may be seen in Figures 5, 8 and 11. When the height is chosen at the center of the box, the ratio of top to bottom detected photons is found to be $\approx 100\%$ in the three cases, meaning that as much photons are captured at the top as at the bottom PMTs.

This distribution is too random (actually, it is a flat distribution in angular direction) when compared to the one followed by cosmic rays, which are the main source of background events. The angular distribution of cosmic ray event directions is best described by a $\cos^2\theta$ function (θ is the zenith angle, varying from $-\pi/2$ to $\pi/2$; angle 0 refers to vertical events). A realization of 100000 events generated according to this distribution is shown in Figure 15, with a fit of the analytical function. Many experimental results confirm this behavior for the cosmic rays flux, except for angles close to $-\pi/2$ and $\pi/2$, where the observed number of events is a bit higher than predicted by the $\cos^2\theta$ distribution.

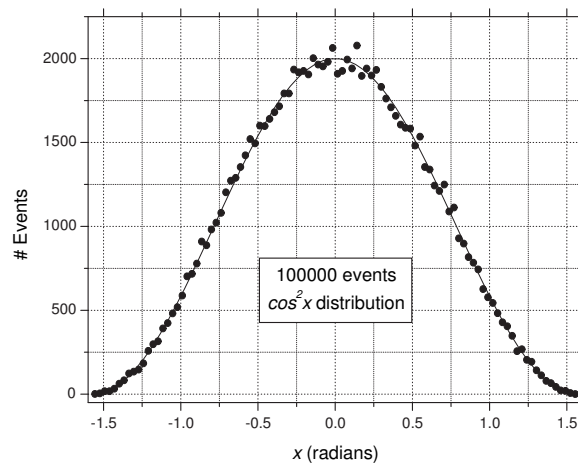


Figure 15: Histogram for events generated according to a $\cos^2(x)$ distribution

When we consider the distribution followed by cosmic rays, the performance of the different configurations is quite different. In Figure 16 are shown the simulation data for the three mentioned configurations of PMTs, for photons arriving from the top surface according to the $\cos^2\theta$ distribution, with up to 10 reflections allowed. The data analysis lead to the following conclusions:

- In the face-to-face PMTs configuration, the photon capture efficiency is $\approx 99\%$, and the fraction of top to bottom photons is $\approx 29\%$;
- In the shifted PMTs configuration, the photon capture efficiency is $\approx 100\%$, and the fraction of top to bottom photons is $\approx 30\%$;

- In the shifted PMTs with reflecting cones configuration , the photon capture efficiency is $\approx 99\%$, and the fraction of top to bottom photons is $\approx 15\%$;

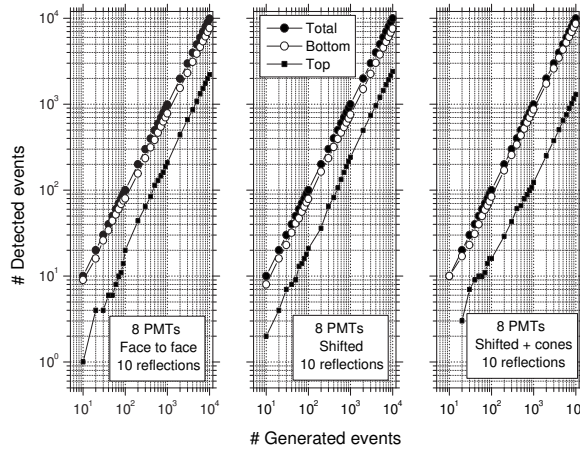


Figure 16: Main results for the three configurations of PMTs around the detecting area.

6 Conclusion

Among the cases treated in this simulation work, the configuration of shifted PMTs with reflecting structures around each of them appears to be the best to provide photon capture efficiency and sensitivity to the incidence direction. This conclusion is valid under the assumption that cosmic rays are the main source of background, and that their directions follow the $\cos^2\theta$ distribution. However, the simulation only dealt with the two-dimensional detector geometry. Not much difference is expected in a three-dimensional computation of tracks, but this task has to be faced, in particular because it will bring more information about the detector performance and validate the mechanical concept. The addition of other features to the software package (*e.g.* photon energy distribution, photocathode quantum efficiency, photon yield for different particles interacting in the target, PMT noise etc.) will generate a realistic tool to evaluate the operation of the central detector.

7 Acknowledgements

The Angra Neutrino Project relies mainly on financial support by FINEP, and also has important contributions from CNPq, FAPERJ, FAPESP, CAPES, and the PCI program of the Ministry of Science and Technology.